Revista Brasileira de Geofísica
RBGf
Brazilian Journal of Geophysics

Revista Brasileira de Geofísica (2012) 30(1): 51-62

ISSN 0102-261X
www.scielo.br/rbg

USING GPR TO IMAGE A TURBIDITE OUTCROP IN ALMADA BASIN, BRAZIL

Marco Antônio Rodrigues de Ceia[1], Antônio Abel González Carrasquilla[1]
and Jandyr de Menezes Travassos[2]

Recebido em 1 novembro, 2011 / Aceito em 12 junho, 2012
Received on November 1, 2011 / Accepted on June 12, 2012

ABSTRACT. Sandy and/or conglomeratic turbidites and shales of Urucutuca Formation outcrops occur in onshore Almada Basin, northeast Brazil. These rocks are part of an exhumed portion of the filling-section of the Almada Canyon, which is well mapped by seismic studies in offshore part. Such outcrops can be considered as analogues to some important turbidite reservoirs of Campos Basin, the main Brazilian petroleum basin. Ground Penetrating Radar (GPR) is an electromagnetic method that can obtain subsurface images with a sub-meter vertical resolution, which is appropriated to study such thin structures usually found in turbidite outcrops. This work shows the results from a set of georadar (GPR) profiles obtained at one outcrop in Almada Basin. Those data yielded high-resolution images of the outcrop, which aided by a geological interpretation of the exposed section and radar 2D forward modeling, could assist on the delineation of channels and layering patterns. That information may prove to be useful in designing more detailed stratigraphical models, which can improve the knowledge of analogues turbidite reservoirs, aiming to enhance the production of oilfields associated to this kind of reservoirs.

Keywords: GPR, Almada Basin, turbidite, outcrops.

RESUMO. Na porção emersa da Bacia de Almada, no sul do estado da Bahia, afloram turbiditos areno-conglomeráticos e folhelhos ricos em foraminíferos planctônicos, os quais definem litoestratigraficamente a Formação Urucutuca. Estas rochas compõem uma grande feição erosiva da seção de preenchimento do cânion de Almada, que é bem definida pelas imagens sísmicas da porção marítima da bacia. Tais afloramentos são análogos a importantes reservatórios turbidíticos da Bacia de Campos. O georadar (GPR) é um método eletromagnético que produz imagens da subsuperfície com resolução vertical submétrica, o que o torna adequado para se estudar as delgadas estruturas geralmente presentes nos afloramentos turbidíticos. Este trabalho visa mostrar os resultados de um conjunto de perfis GPR obtidos em um dos afloramentos da Bacia de Almada. Estes dados geraram imagens de alta resolução do afloramento, as quais, com o auxílio da interpretação geológica da face exposta e de uma modelagem direta 2D, possibilitaram o delineamento de canais e padrões de acamadamento. Estas informações podem ser úteis na elaboração de modelos estratigráficos detalhados, que possam aprimorar o conhecimento acerca dos sistemas de reservatórios turbidíticos análogos, e posteriormente orientar as estratégias para aumentar a produção de campos de petróleo associados a esse tipo de reservatório.

Palavras-chave: georadar, Bacia de Almada, turbiditos, afloramentos.

[1]Petroleum Engineering and Exploration Laboratory (LENEP), Universidade Estadual do Norte Fluminense Darcy Ribeiro (UENF), Rodovia Amaral Peixoto, Km 163, Av. Brennand, S/N – Imboassica, 27925-535 Macaé, RJ, Brazil. Phone: +55 (22) 2773-8032; Fax: +55 (22) 2765-6577 – E-mails: marco@lenep.uenf.br; abel@lenep.uenf.br

[2]MCT/Observatório Nacional, Rua General José Cristino, 77, São Cristóvão, 20921-400 Rio de Janeiro, RJ, Brazil. Phone: +55 (21) 3878-9100; Fax: +55 (21) 2580-6041 – E-mail: jandyr@on.br

INTRODUCTION

More than 80% of all the petroleum in Brazil is produced from turbidite reservoirs, mainly in Campos Basin. In that kind of reservoirs many of the geological features that control petroleum production are smaller than the resolution of typical seismic reflection surveys. Outcrops of reservoir analogues fill that scale gap allowing a more detailed study and producing data that can be translated into porosity and permeability architectural models (Young et al., 1999, 2001; Pringle et al., 2010). Accurate models can lead to new discoveries or an enhancement of oil recovery in producing fields by means of an optimized well location strategy to avoid flow barriers such as facies changes and small-scale structural discontinuities.

Ground Penetrating Radar (GPR) is a very efficient geophysical technique to study shallow subsurface sediments due to its high-resolution images of the sedimentary architecture (Liner & Liner, 1995; McMehan et al., 1997; Staggs et al., 2003). GPR is based on the reflections of electromagnetic waves caused by changes in the electromagnetic properties of subsurface associated to changes in lithology or water content. Although that high-resolution makes this method extremely useful in outcrop studies (McMehan et al., 1997; Pringle et al., 2000; Van den Bril et al., 2007), it is also associated to a relatively low signal penetration that limits its depth of investigation. More details of this method can be found in Davis & Annan (1989) and Annan (1992).

Typical depth of investigation with a central frequency of 100 MHz is in the range of 10-15 m (Annan, 1992). GPR method has been widely used for high-resolution imaging of internal structure of reservoir analogues. Good references for GPR imaging of sandstone analogues can be found in: McMehan et al. (1997), Van den Bril et al. (2007) and Akinpelu (2010); while for carbonate analogues can be found in: Jeannin et al. (2006) and Pipan et al. (2010). In Brazil, GPR was also successfully used to image such sandstones (Porsani & Rodrigues, 1999) as carbonates (Takayama et al., 2009).

In general, GPR surveys are conducted on the top of the outcrops, thus allows a comparison between the radar sections and a visual (photographic) interpretation of the cliff face. 3D surveys can provide a better understanding of the spatial orientation of channels, faults and heterogeneities. Sometimes it is possible to run vertical surveys along the cliff (Jeannin et al., 2006) resulting in a more accurate depth correlation between the radar sections and photo-interpretation. GPR images are often combined with: aerial or ground-based digital photogrammetry and digital topographic models (obtained from reflectorless total station or differential GPS), for integrated interpretation (Pringle et al., 2006). In recent years a new technology, called LIDAR (Light Detection and Ranging) that uses a laser scanner to produce virtual 3D models of the outcrops has been very used (Teixeira, 2008).

Channel geometry, continuity and connectivity were well imaged by both 2D and 3D GPR surveys, yielding models of the architectural framework of some US outcrops (Young et al., 1999, 2001; Staggs et al., 2003). Pringle et al. (2001) used GPR to measure 3D architecture in a turbidite channel system, the Carboniferous Ross Formation, in Ireland. They investigated a variety of frequencies in order to image the turbidite channel margins, bedding geometry and fine-scale sedimentological changes. Pringle et al. (2010) created 3D digital models of submarine channel complex in South Africa, through the integration of GPR, LIDAR and photogrammetry data.

In spite of the fact that there is no turbidite outcrop in the onshore portion of Campos Basin, we can use the contemporaneous and geologically similar Almada Basin turbidite outcrops. In this paper we use 2D and 3D GPR images combined with a 2D radar forward model of the cliff face to characterize the channel geometry and continuity of one the Almada Basin outcrops.

GEOLOGY

Almada Basin is a passive margin basin on northeast coast of Brazil, situated between 14°15′S and 14°55′S, limited by the Itacaré High on its Northern limits and by the Olivença High on the south. It has a small onshore portion, which spreads out over 200 km^2 with a maximum sedimentary thickness of 1,800 m. The larger offshore portion spreads out over roughly 1,300 km^2 reaching 200 m below sea level with a maximum sedimentary thickness over 6,000 m.

Early geological studies of the onshore portion in the 60's revealed sandy and/or conglomeratic turbidites and planktonic foraminifera shales outcrop related to the Urucutuca Formation (Carvalho, 1965). Those Mesozoic/Upper Cretaceous geological features are an exhumed part of the filling-section of the Almada Canyon, a huge erosive feature, which is seismically well mapped in offshore portion (Bruhn & Moraes, 1989). Bruhn & Moraes (1989) and Mendes (1998) presented detailed studies of the outcrops, analogues to other formations found in Campos, Espírito Santo and Cumuruxatiba Basins. As a matter of fact several oilfields, like Carapeba, Enchova and Pargo in Campos Basin and Lagoa Parda, Fazenda Alegre, Fazenda Cedro and Fazenda Queimadas in Espírito Santo Basin are all associated to that type of paleostructure.

The early studies mentioned above associated some observed channels on the turbidite outcrops of the main Urucutuca Formation to channel-levees/overbanks. Figure 1, modified from the

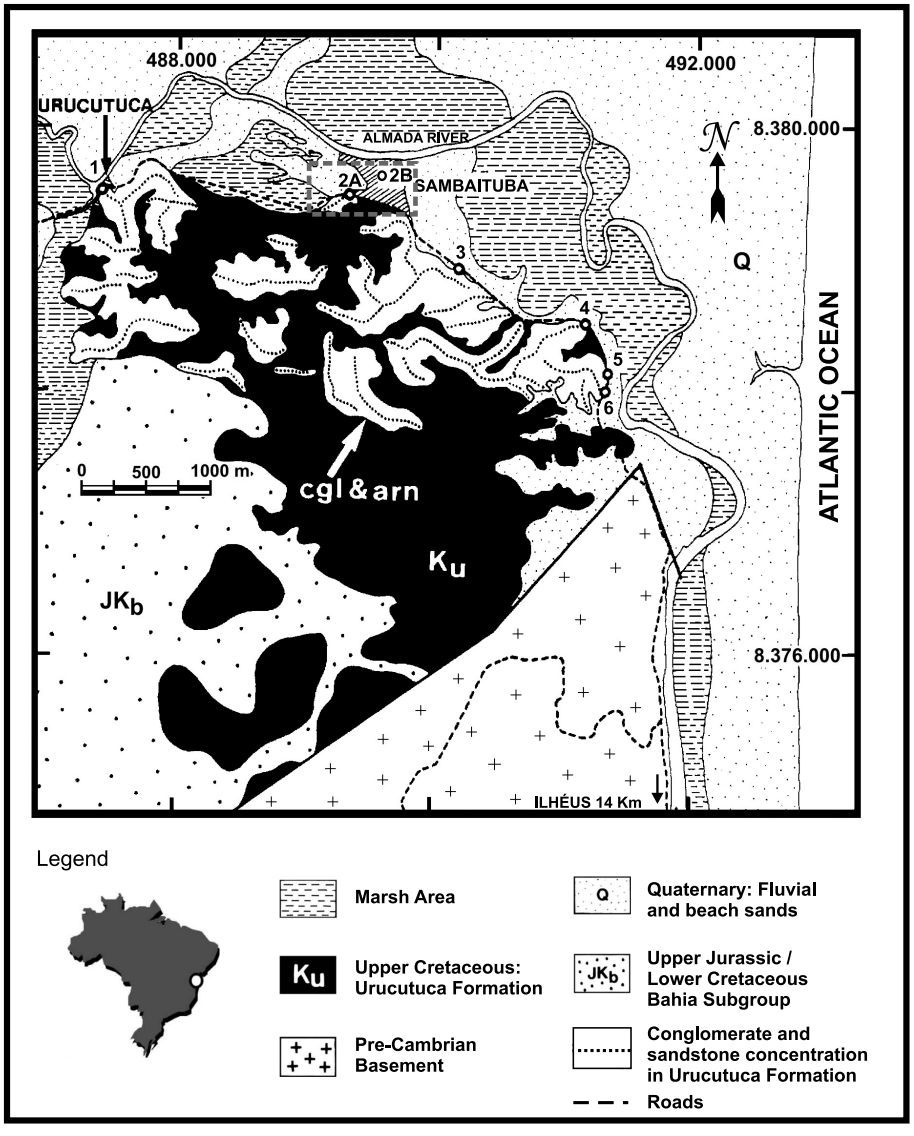

Figure 1 – Map showing the position of main outcrops of Urucutuca Fm. (labelled as 1 to 6). The grey dashed rectangle shows the study area (outcrops 2A and 2B). After Bruhn & Moraes (1989).

literature (Bruhn & Moraes, 1989) gives the location of those outcrops, which are labeled as 1 to 6. Later a new outcrop (2B) was found (Dias et al., 2004a).

The origin of the Almada Canyon can be related to the movement of ancient strike-slips basement faults during the Cretaceous later re-activated as normal (gravity) faults during the deposition of Urucutuca Formation that created a submarine conduct from the continent to the deepwater portion (D'Ávila et al., 2004). Several fluvial discharges on that submarine depression created flows and hyperpicnal floods that ran through the continental shelf as turbidity currents, giving rise to intensive erosion of substrata and transporting huge volume of sediments to the basin. Part of that load was deposited in the canyon creating turbidite channels filled by conglomerates and sandstones. The turbidites are intercalated by prodelta pelites and deposits of low density turbid plumes, which have mostly been re-mobilized as slumps and debris flows. Major accumulation of the pelites occurred during normal fluvial sedimentation phases, when the sandy sediment was retained in the canyon head and reworked by tides on the upper part of the estuary (D'Ávila et al., 2004).

Very few geophysical works has been done on the turbidite outcrops up to this time. Some new stratigraphical and structural interpretation was provided by an earlier study that reported on new geological and geophysical datasets (Dias et al., 2004a).

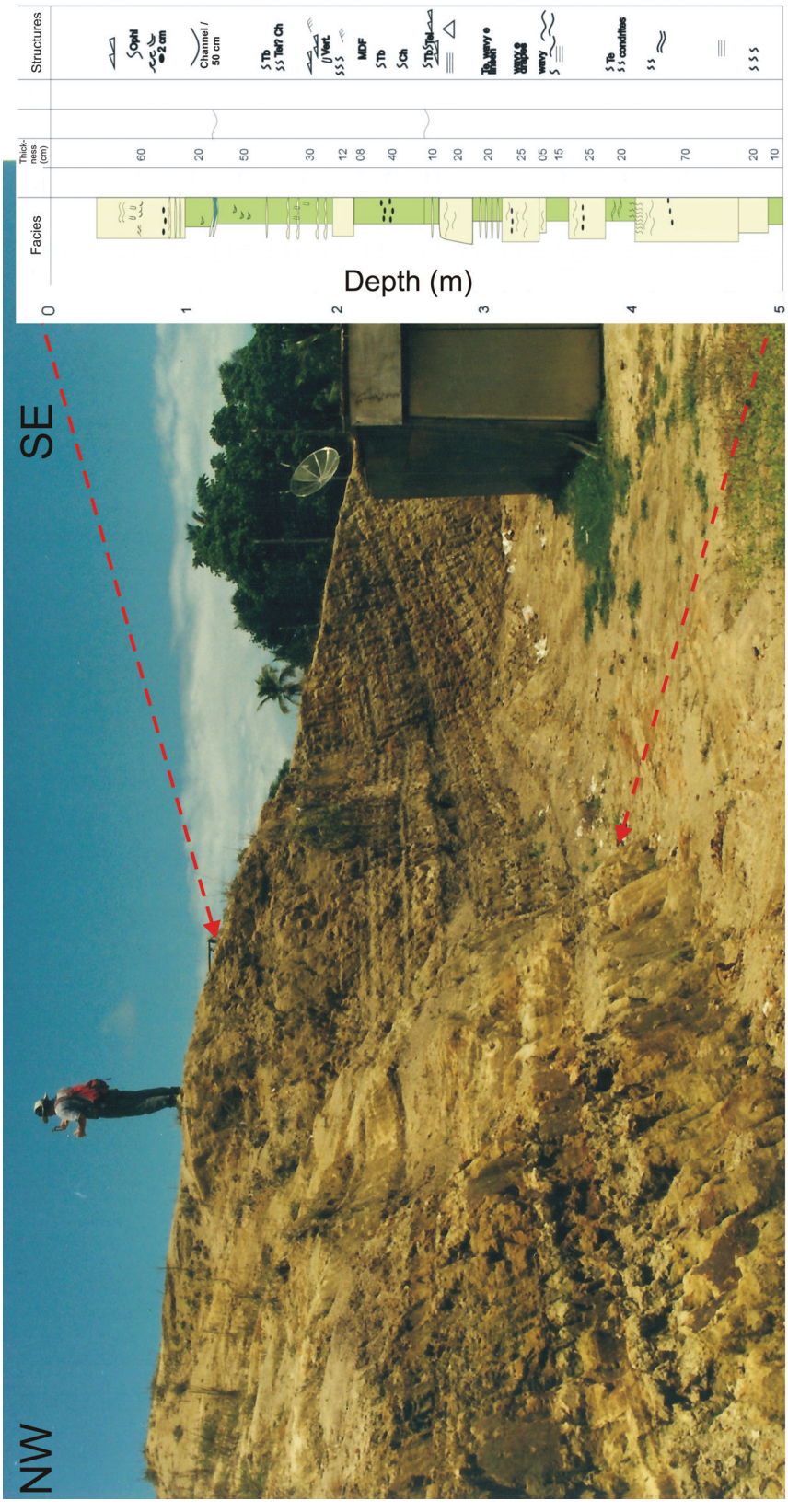

Figure 2 – Photograph of outcrop 2B. The cliff face is approximately NW-SE and exhibits an intercalation of silts and sandstones. A geological description of a vertical column along the cliff face (D'Ávila et al., 2004) is also showed on the right side.

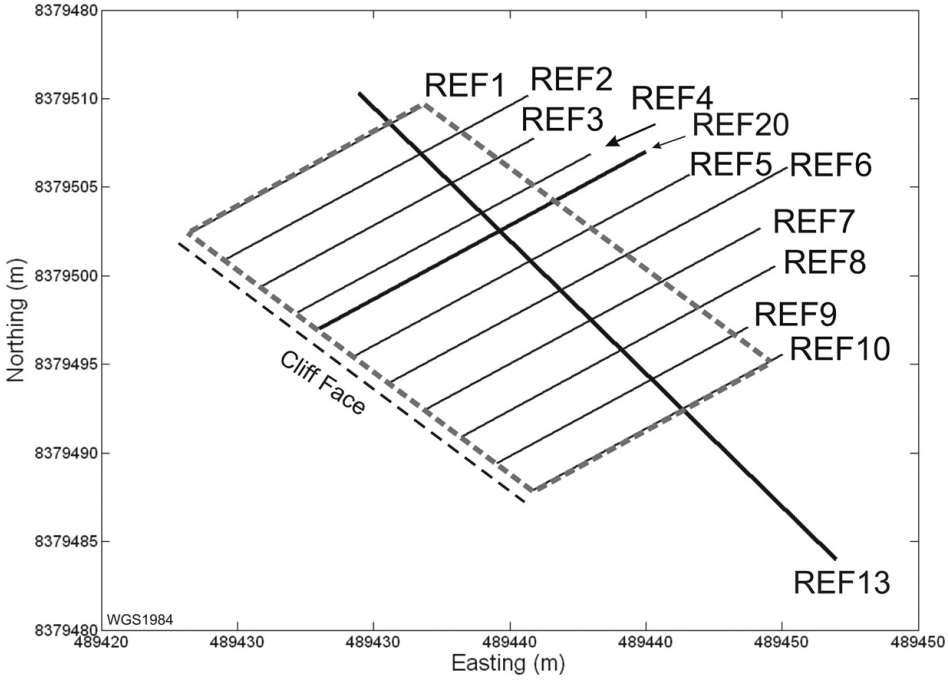

Figure 3 – Map of the location of the GPR profiles (solid lines) obtained on outcrop 2B. The grey dashed rectangle indicates part of the data used for 3D interpolation. The cliff face is indicated as a black dashed line. REF13 and REF20 are the profiles to be used in a fence diagram.

This work will add some new light on one of the outcrops, the one marked as 2B in Figure 1, which displays silts and sandstones as its two main lithologies as shown in Figure 2 (D'Ávila et al., 2004).

FIELDWORK

The field survey was carried out on the 3 outcrops labeled 2A, 2B and 3 in Figure 1. Results from outcrop 2A are reported in the literature (Ceia et al., 2004). Here we shall restrict to the data obtained in outcrop 2B. A total of 14 GPR profiles (13 fixed-offset and a single common mid-point (CMP)) were done on that outcrop (Fig. 3). We used a PulseEKKO IV GPR system with 100 MHz antennas in all profiles. Time window and station spacing were set to 300 ns and 0.25 m respectively. Fixed offset spatial sampling was 0.1 m and the CMP was done in steps of 0.2 m until a final offset of 25.4 m. Positioning was obtained with a Trimble DGPS post-processed system with accuracies smaller than 0.1 m (horizontal) and 0.2 m (vertical). A portable clinometer was used to provide a relative topography along profiles.

DATA PROCESSING

Data processing was done using Seismic Unix, GRADIX and Sensors & Software EkkoTools. It included Trace Editing, Dewow, Time-zero Correction, Time-window Limitation, SEC gain, Velocity Analysis, Stolt F-K Migration, Band-Pass Time Filtering and Elevation Correction. A band-pass filter with 30-70-180-500 MHz cutoff frequencies was applied in order to eliminate unwanted noise mainly at low frequencies. Spectral balancing was also applied prior to migration in order to reduce the combined effects of dispersion and absorption in the GPR signal attenuation (Xavier Neto & Medeiros, 2003). F-K dip filtering (Yilmaz, 1987) was used to minimize ringing due to a nearby metallic fence that appeared in the sections as steeply dipping events.

Figure 5 shows the CMP data together with the velocity analysis. It is possible to note the presence of high velocity air waves along the whole time window. The best estimate for the velocity is $v = 0.1$ m/ns, later confirmed at the migration stage. This velocity was used for Stolt Migration, elevation correction and time-to-depth conversion. The maximum penetration depth in the outcrop was $\sim$15 m.

INTERPRETATION

We concentrate our discussion on two perpendicular profiles REF13 and REF20 shown in Figure 4. This figure shows a relatively blank zone in the first meter (REF13), followed by a couple of meters of sub parallel layers probably thin-bedded sand and shale layers. The sections become more structured below 4 m, showing the presence of channels. There is a strong evidence of a sandstone channel at 150-200 ns (red rectangle). The oblique

features with similar dips are bounded by two reflectors that separate regions of different facies and geometries.

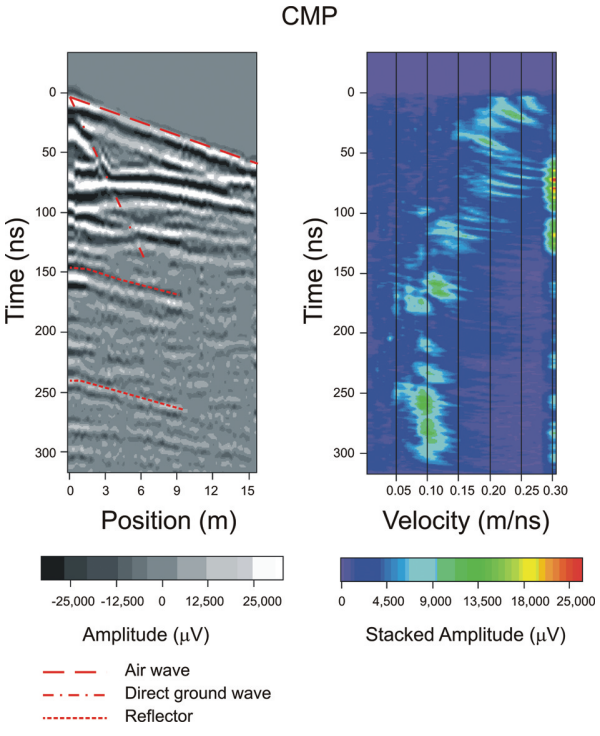

Figure 4 – Velocity analysis of the CMP profile carried on outcrop 2B. The left panel shows the CMP section and the right panel the velocity spectrum.

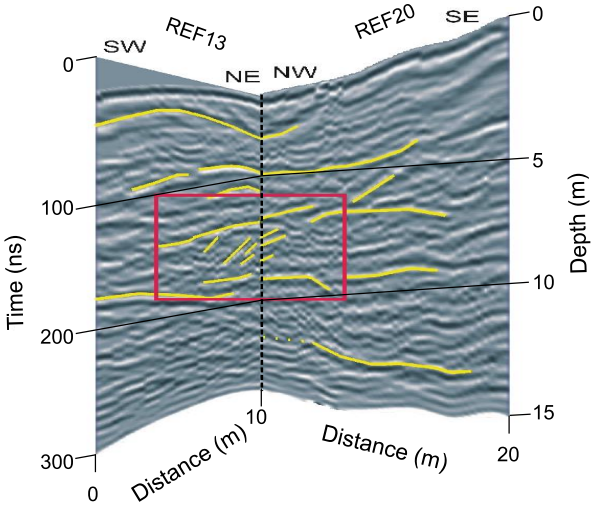

Figure 5 – Fence diagram of profiles REF13 (left side) and REF20 (right side). For a constant velocity of 0.1 m/ns, it can be said that 100 ns = 5 m. Red rectangle indicates a sandstone channel.

Figure 6 shows a comparison between the first 5 m of profile REF13 and the exposed section. There is a good agreement between the GPR data and the layering features observed at the digital photographs. Plain-parallel structures onlap an arched feature that dips to NW, probably a signature of a small channel. However, at the end of the profile (from 23 to 31 m) there are plain-parallel structures which dip to SE instead of NW. That inversion is not observed at the exposed section, and maybe it should be associated to a deeper anticline structure which tends to pull up the upper layers.

We have used the 2D forward modeling code GPRMAX (Giannopoulos, 2002) to test some of our interpretation hypothesis through the comparison between the synthetic and real data images. The GPRMAX code solves Maxwell's equations using finite-difference time domain method (FDTD) (Giannopoulos, 1997). The model shown in Figure 7 was built based on photographs and geological description of the outcrop (Fig. 2). The synthetic radargram obtained through 2D forward modeling shown in Figure 8 uses the same station spacing and central frequency of real data and discretization steps of 0.05 m in both distance and depth. The source excitation is a Ricker wavelet.

Only two lithologies were considered as media, silts ($\sigma = 1$ mS/m $\varepsilon'_r = 15$) and sandstones ($\sigma = 0.1$ mS/m $\varepsilon'_r = 9$), where σ is the real part of the conductivity and ε'_r the relative electrical permittivity. Those values were chosen based in information from cores obtained from a nearby borehole (Dias et al., 2004b). The main reflectors observed in real data (Fig. 6) also are also present in the synthetic radargram indicating a good overall match. Plain-parallel and cross-bedding structures are also in a relatively a good agreement for both sections. The inclusion of two relatively blank zones (low contrast zones) at the beginning and at the end of the profile was based on observation of the real data. The main differences between the two images are probably due to variations in water content along the profile and smaller scale structures.

We now extend our analysis to the whole dataset of 12 fixed-offset profiles. All profiles but REF13 run transversal to the cliff face (NE-SW), please refer to Figure 3. As we want results parallel to the cliff face we generate cross-line sections through interpolation of the transverse profiles by a special *adhoc* linear interpolation algorithm. The cross-lines were interpolated with a grid size equal to half step size, i.e., 1 m. Grid size in time (depth) and in-line directions was equal to time and spatial sampling, thus with no interpolation. The reader should be aware of the difference in polarization between the interpolated cross-lines and profile REF13 (Travassos et al., 2008).

The pseudo-3D cube is shown in Figure 9, in which it can be seen a lateral view of the shallow channel. This cube can also be used to attempt tracking the observed channel in the 2D cross-

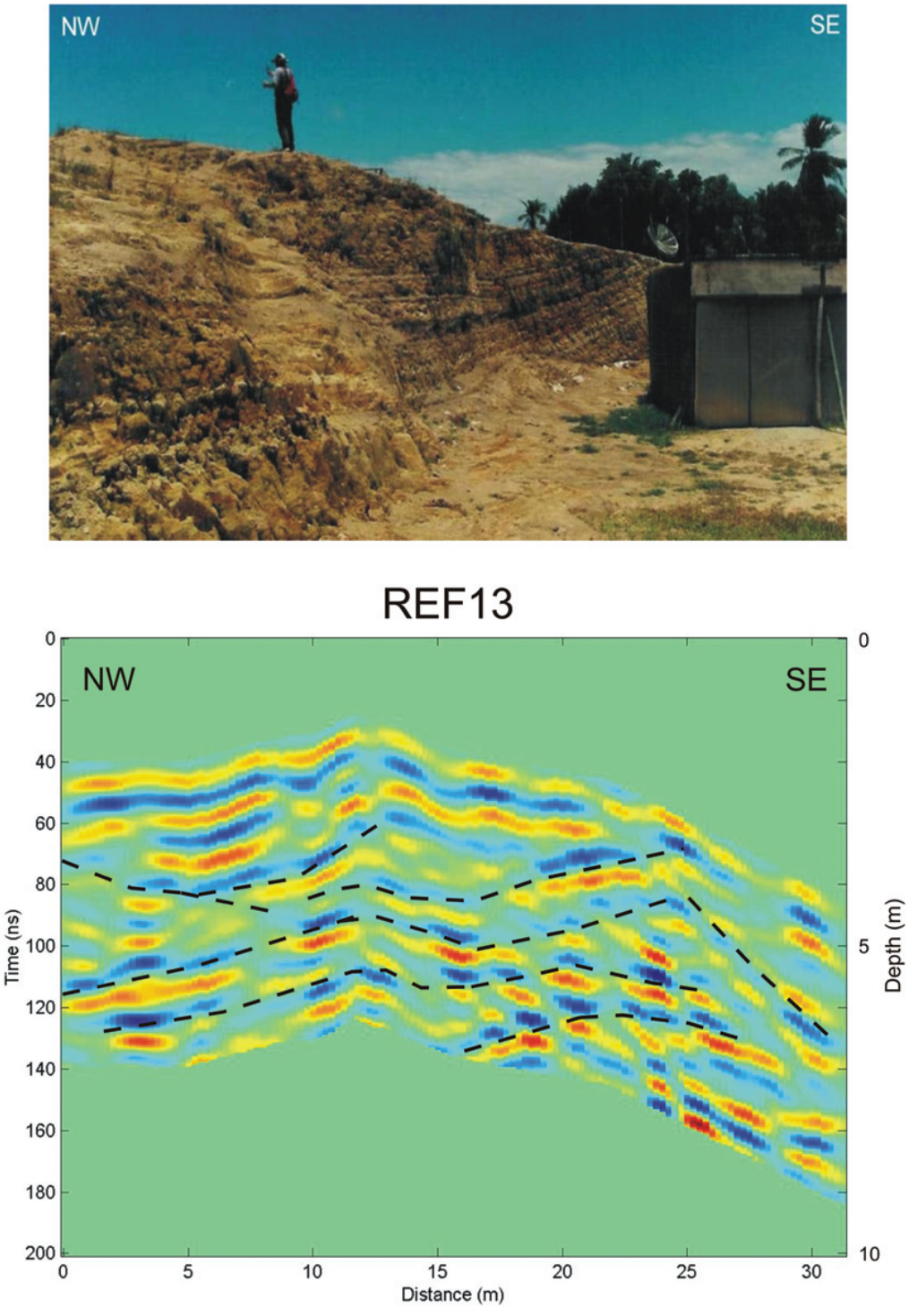

Figure 6 – The upper panel shows a photograph of outcrop 2B and the lower panel a section of REF13, limited to the first 5 m. The dashed lines indicate the main observed structures.

sections (Fig. 10A) as well as to assign an isosurface linking all 2D interpretations thus rendering a 3D shape for that channel (Fig. 10B). In that we also use the outcrop photograph to guide channel's delineation throughout the cross-lines. The resulting image revealed that it has 2.5 m maximum depth and about 10 m in width. Its transversal axis is NE-SW.

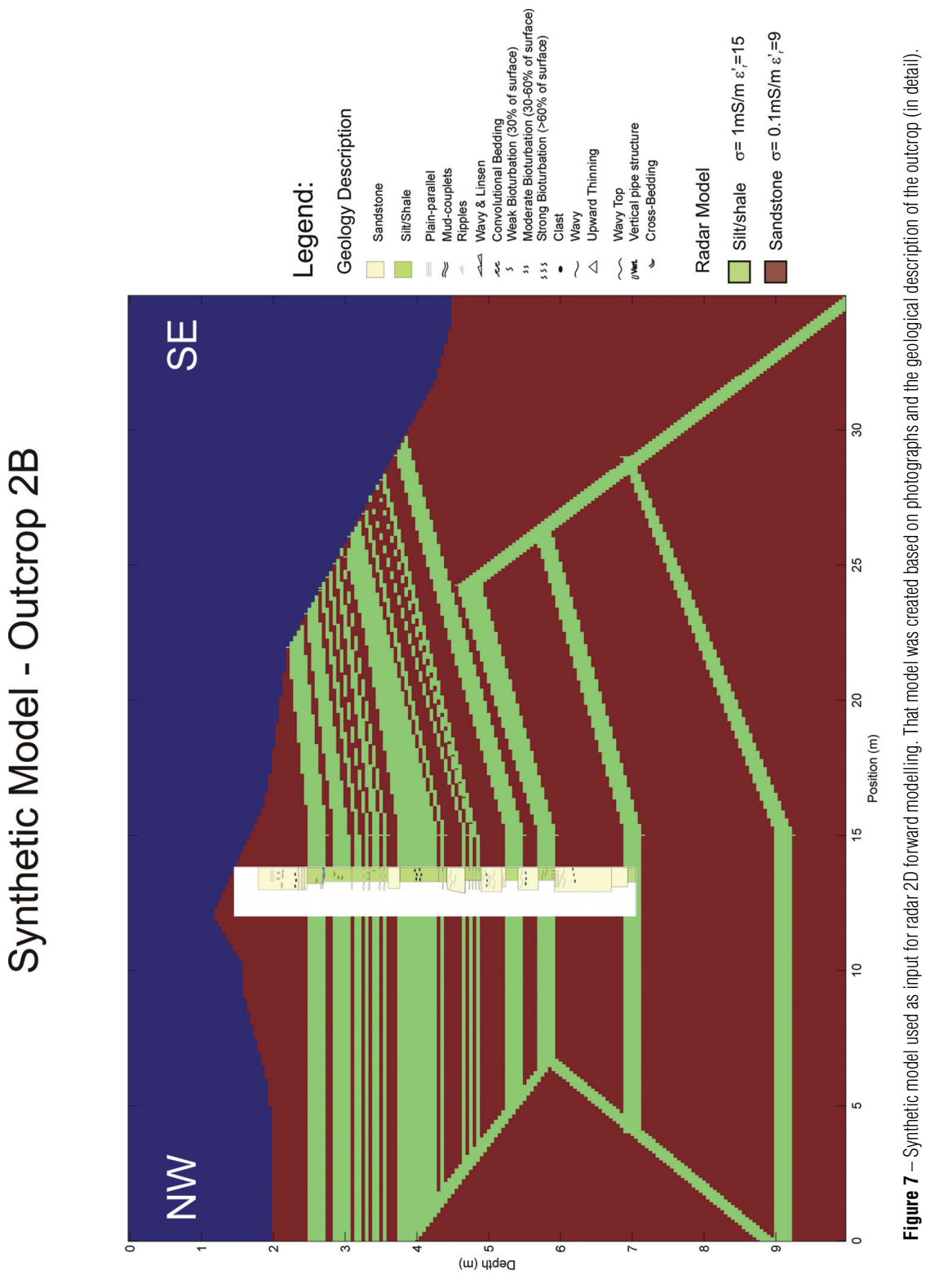

Figure 7 – Synthetic model used as input for radar 2D forward modelling. That model was created based on photographs and the geological description of the outcrop (in detail).

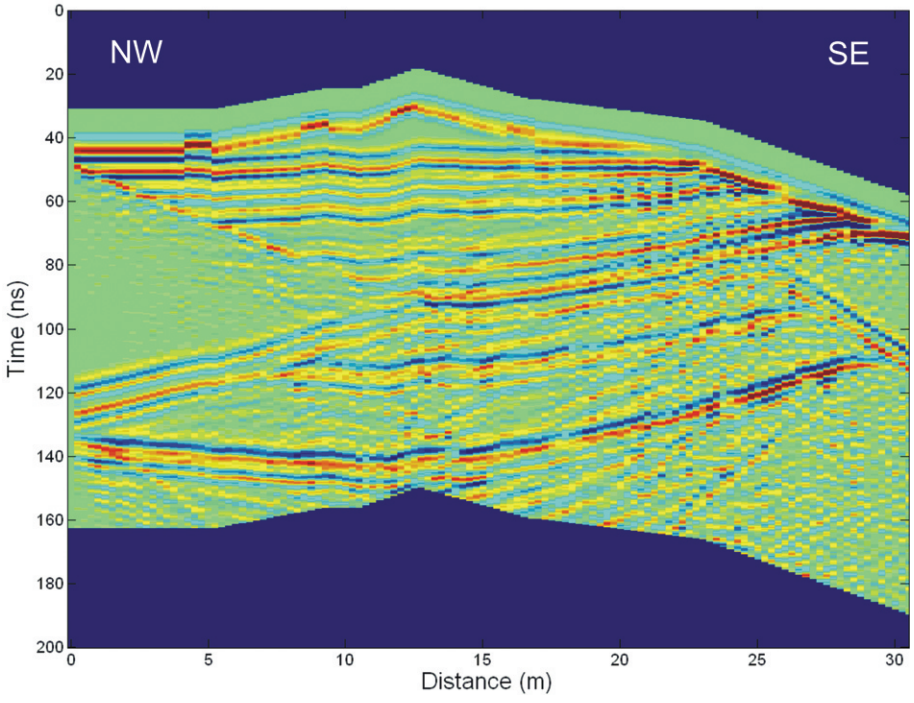

Figure 8 – Radargram obtained through a radar 2D forward modelling using the model showed in Figure 7.

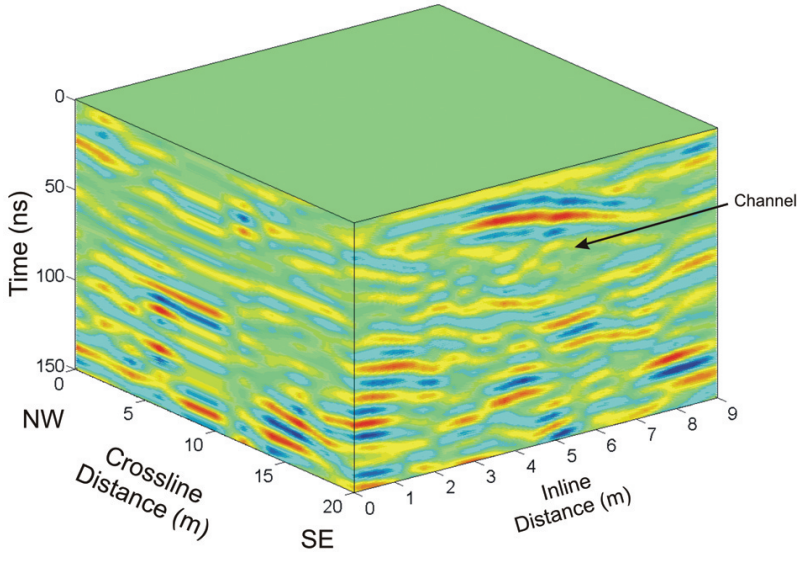

Figure 9 – 3D view provided by 3D interpolation of GPR profiles. A lateral view of the shallow channel can be observed in the in-lines.

The oblique features observed in radargrams of outcrop 2B are similar to those observed in radargrams of outcrop 2A (Ceia et al., 2004), but in opposite directions, i.e., in outcrop 2A, the channel basement is characterized by an oblique feature dipping to SE, while in outcrop 2B the observed oblique feature dips to NW. Unfortunately no data is available in the region between the two outcrops. Transversal axis, in both outcrops is approximately NE-SW, which is the same direction of the main fault system of that region (Bruhn & Moraes, 1989). The onlap layering pattern could be seen in both outcrops, probably as result of shale or silt thin-bedding in sandstone layers.

All of those features are very similar to those reported by D'Ávila & Paim (2003) for hyperpicnal turbidite models. It should be noticed that in this layering configuration, the sandstone

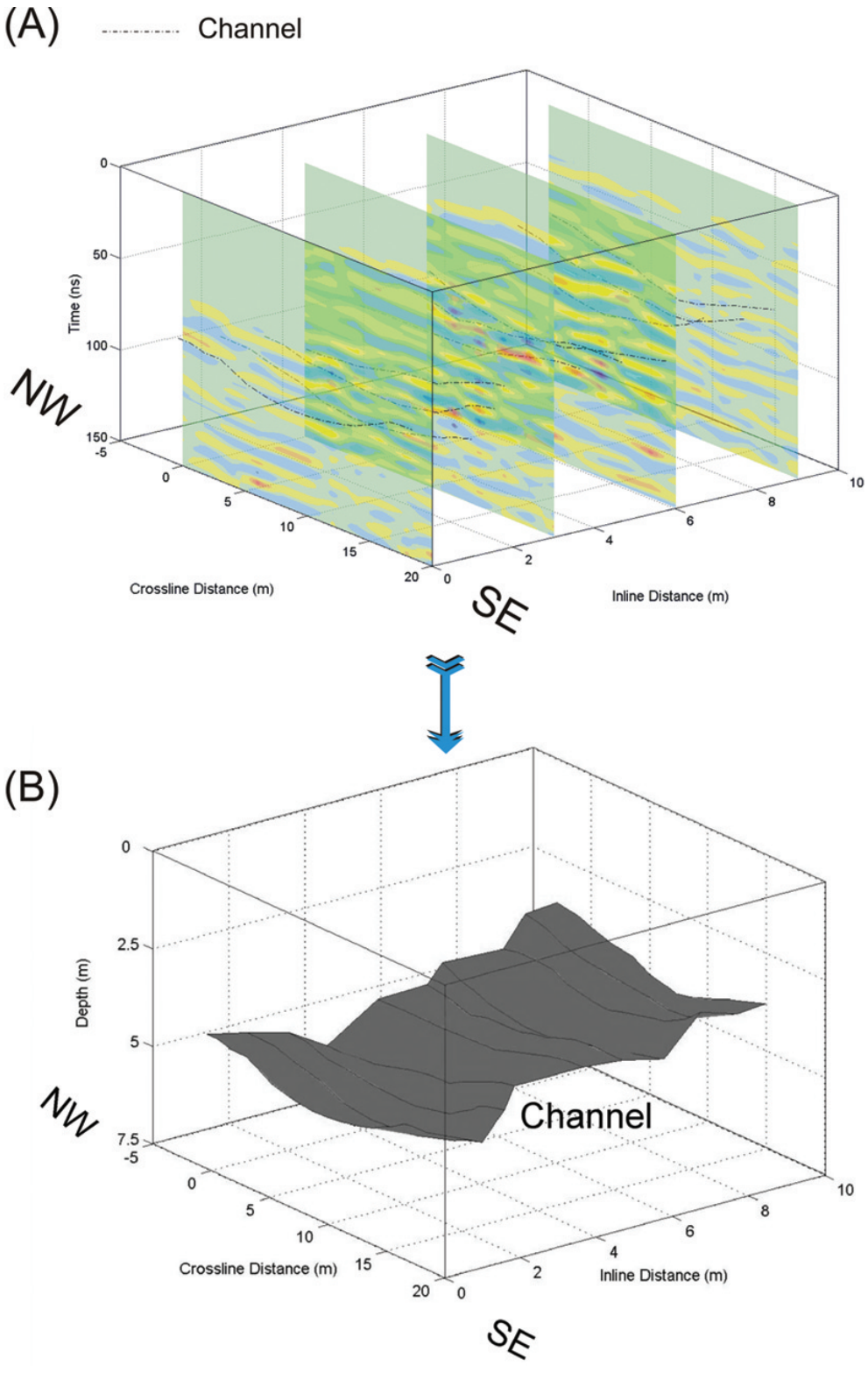

Figure 10 – (A) Cross-sections generated by a 3D interpolation of 11 profiles acquired on outcrop 2B. Transparency was set to 50%. The dash-dot lines indicate a sandstone channel mapped on several cross-slices. (B) Basement of the channel revealed after assigning a surface to link each 2D interpretation.

trapped by thin-bed shales (or silts) can work as a reservoir and the faults can function as a migration path. Some of those structures can be thinner as 5 m or even sub-metric, but depending on how large are the layers, these information can be very useful when modeling that type of reservoirs.

CONCLUSION

The GPR method has been very successful revealing some stratigraphic features of Almada Basin turbidite outcrops, like channels and bedding patterns, which were visible on the cliff face. A 2D radar forward modeling of the cliff face was applied to check the continuity and lateral geometry of those structures through a qualitative comparison between the synthetic and the observed sections. The resulting model shows plain-parallel layers of silts and sandstones, and a small shallow channel.

The geometry of that shallow channel could be delineated after the 3D interpolation of a set of radar sections, which provided pseudo-3D images that proves to be very useful for mapping the spatial distribution of such geological structure. Those images showed that the direction of the transversal axis of that channel is the same of the channel observed in outcrop 2A, and it is also coincident to the direction of the main fault system of that region.

The results brought new information about the structural features of Urucutuca Fm. outcrops and help to improve the knowledge of the depositional system of the main reservoir of Almada Basin.

ACKNOWLEDGEMENTS

The research leading for this paper was funding by CTPETRO. JMT and AAGC thank CNPq for research fellowships. We also thank Carlos A. Dias and Roberto D'Ávila ("Turbiditos" project coordinators) for their support.

REFERENCES

AKINPELU O. 2010. Ground Penetrating Radar Imaging of Ancient Clastic Deposits: A Tool for three-dimensional Outcrop Studies. Ph.D. Thesis. Geology Department. University of Toronto. Canada. 295 pp.

ANNAN AP. 1992. Ground Penetrating Radar workshop notes. Sensors & Software Inc. 129 pp.

BRUHN C & MORAES M. 1989. Turbiditos da Formação Urucutuca na Bacia de Almada, Bahia: um Laboratório de Campo para Estudo de Reservatórios Canalizados. Boletim de Geociências da Petrobras, 3(3): 235–267.

CARVALHO KWB. 1965. Geologia da Bacia Sedimentar do Rio Almada. Boletim Técnico da Petrobras, 8(1): 5–55.

CEIA MAR, CARRASQUILLA AAG & TRAVASSOS JM. 2004. Levantamento GPR em Afloramentos Turbidíticos da Bacia de Almada – BA. Revista Brasileira de Geociências, 34(3): 411–418.

D'ÁVILA RSF & PAIM PSG. 2003. Mecanismos de Transporte e Deposição de Turbiditos. In: PAIM, PSG, FACCINI UF & NETTO RG (Eds.). Geometria, arquitetura e heterogeneidades de corpos sedimentares – Estudos de casos. UNISINOS – São Leopoldo – RS. p. 93–121.

D'ÁVILA RSF, SOUZA-CRUZ CE, OLIVEIRA FILHO JSO, JESUS CM, CESERO P, DIAS FILHO DC, LIMA CC, QUEIROZ CL, SANTOS SF & FERREIRA EA. 2004. Fácies e Modelo Deposicional do Canyon de Almada. In: DIAS CA, THOMAZ FILHO A & D'ÁVILA RSF (Eds.). Turbiditos da Bacia de Almada/Pesquisas Geológicas e Geofísicas. FAPERJ. 2.2: 41–69.

DAVIS JL & ANNAN AP. 1989. Ground-Penetrating radar for high-resolution mapping of soil and rock stratigraphy. Geophys. Prosp., 37: 531–551.

DIAS CA, THOMAZ FILHO A & D'ÁVILA RSF. 2004a. Turbiditos da Bacia de Almada/Pesquisas Geológicas e Geofísicas. FAPERJ, 150 pp.

DIAS CA, SILVA DN, CARAGEORGOS T & LENHARO SLR. 2004b. Condutividade Elétrica Espectral em Testemunhos de Poços (SST – 1 e 2) Perfurados nos Turbiditos de Almada, BA. In: DIAS CA, THOMAZ FILHO A & D'ÁVILA RSF (Eds.). Turbiditos da Bacia de Almada/Pesquisas Geológicas e Geofísicas. FAPERJ. 3.4: 119–132.

GIANNOPOULOS A. 1997. The investigation of Transmission-Line Matrix and Finite-Difference Time-Domain Methods for the forward Problem of Ground Penetrating Radar. D. Phil. Thesis, Department of Electronics, University of York. UK. 189 pp.

GIANNOPOULOS A. 2002. GPRMAX2D User's Manual version 1.5. 67 pp.

JEANNIN M, GARAMBOIS S, GRÉGOIRE C & JONGMANS D. 2006. Multiconfiguration GPR measurements for geometric fracture characterization in limestone cliffs (Alps). Geophysics, 71(3): B85–B92.

LINER CL & LINER JL. 1995. Ground-penetrating radar: A near-face experience from Washington County, Arkansas. The Leading Edge, 14: 17–21.

McMEHAN GA, GAYNOR GC & SZERBIAK RB. 1997. Use of ground-penetrating radar for 3D sedimentological characterization of clastic reservoir analogs. Geophysics, 62: 786–796.

MENDES MP. 1998. Evolução, análise estratigráfica e sistemas turbidíticos em paleocânions submarinos: exemplos de Almada (BA) e Regência (ES). M.Sc. Dissertation, UFRGS, Porto Alegre, 229 pp.

PIPAN EF, CASABIANCA D, DI CUIA R & RIVA A. 2010. 2D and 3D GPR imaging and characterization of a carbonate hydrocarbon reservoir analogue. In: 13th International Conference on Ground Penetrating Radar (GPR). Lecce. Italy. CD-ROM.

PORSANI JL & RODRIGUES ARR. 1999. O Método GPR aplicado à Caracterização de Reservatórios: Um exemplo no Afloramento Açu – Bacia Potiguar – RN. In: V Congresso Internacional da Soc. Bras. de Geofísica. Rio de Janeiro-RJ. Expanded Abstracts, CD-ROM.

PRINGLE JK, WESTERMAN AR, CLARK JD, GARDINER AR & CORBERTT PWM. 2000. 3D GPR surveying with vertical Radar Profiling (VRP) of petroleum reservoir outcrop analogues. In: Proceedings of the 62nd EAGE Conference & Technical Exhibition, Glasgow, Scotland. Expanded Abstracts, CD-ROM.

PRINGLE JK, WESTERMAN AR, CLARK JD & GARDINER AR. 2001. Ground Penetrating Radar (GPR) used to measure 3D architecture in the Carboniferous Ross Formation, County Clare, Western Ireland. In: EAGE 63rd Conference and Technical Exhibition. Amsterdam, The Netherlands. Expanded Abstracts, CD-ROM.

PRINGLE JK, HOWELL JA, HODGETTS D, WESTERMAN AR & HODGSON DM. 2006. Virtual outcrop model of petroleum reservoir analogues: a review of the current state-of-art. First Break, 24: 33–42.

PRINGLE JK, BRUNT RL, HODGSON DM & FLINT SS. 2010. Capturing stratigraphic and sedimentological complexity from submarine channel complex outcrops digital 3D models, Karoo Basin, South Africa. Petroleum Geoscience, 16: 307–330.

STAGGS JG, YOUNG RA & SLATT RM. 2003. Ground-penetrating radar facies characterization of deepwater turbidite outcrops. The Leading Edge, 22: 888–891.

TAKAYAMA P, MENEZES PTL & TRAVASSOS JMT. 2009. 3D GPR Modelling of Carbonates Reservoir Analogues Applying Geometric Attributes: Coqueiro Seco Formation, Sergipe-Alagoas Basin-Brazil. In: XI International Congress of the Brazilian Geophysical Society. Salvador-BA. Expanded Abstracts, CD-ROM.

TEIXEIRA WLE. 2008. Aquisição e construção de modelos estáticos análogos a reservatórios petrolíferos com tecnologia LIDAR e GEORADAR. M.Sc. Dissertation, Petroleum Engineering Postgraduate Program, Universidade Federal do Rio Grande do Norte. 99 pp.

TRAVASSOS JM, ANDRÉ S & MUSA JE. 2008. A Multi-component GPR Survey in Marambaia Isthmus. Near Surface Geophysics, 6: 269–275.

VAN DEN BRIL K, GREGOIRE C, SWENNEN R & LAMBOT S. 2007. Ground Penetrating radar as a tool to detect rock heterogeneities (channels, cemented layers and fractures) in Luxembourg Sandstone Formation (Grand Duchy of Luxembourg). Sedimentology, 54: 949–967.

XAVIER NETO P & MEDEIROS WE. 2003. Uma abordagem prática para corrigir os efeitos de propagação no sinal GPR, e sua importância na melhoria do imageamento. In: 8th International Congress of the Brazilian Geophysical Society. Rio de Janeiro, Brazil. Expanded Abstracts, CD-ROM.

YILMAZ O. 1987. Seismic Data Processing. Society of Exploration Geophysicists. Tulsa, OK, USA. 526 pp.

YOUNG RA, PETERSON B & SLATT RM. 1999. Imaging of Turbidite Outcrop Analogs Using Ground Penetrating Radar. In: 69th Annual Meeting: Soc. Expl. Geophys., p. 429–432.

YOUNG RA, STAGGS J, SLATT RM & HURLEY NF. 2001. Turbidite Outcrop 3D Ground Penetrating Radar Imaging: Lewis Shale, WY. In: 71st Annual Meeting: Soc. Expl. Geophys., 1592-1595. Expanded Abstracts, CD-ROM.

NOTES ABOUT THE AUTHORS

Marco Antônio Rodrigues de Ceia received a B.Sc. in Physics from Universidade Federal do Rio de Janeiro-UFRJ (1994), a M.Sc. in Geophysics from Observatório Nacional (1997) and a D.Sc. in Reservoir and Exploration Engineering from Universidade Estadual do Norte Fluminense-UENF (2004). Currently is Associate Professor of the Petroleum Engineering and Exploration Laboratory (LENEP) at UENF working on Petrophysics, Seismic Physical Modeling and Applied Geophysics.

Antonio Abel González Carrasquilla received a B.Sc. in Chemistry from Universidad Nacional de Panama (1979), a M.Sc. (1984) and a D.Sc. (1993) in Geophysics from Universidade Federal do Pará. Specialist in electromagnetic methods for natural resources prospecting, mainly groundwater and oil. Presently is Full Professor of the Petroleum Engineering and Exploration Laboratory (LENEP) at Universidade Estadual do Norte Fluminense-UENF, Brazil.

Jandyr de Menezes Travassos is a senior researcher at the Observatório Nacional, Rio de Janeiro, since 1977. Holds a Bachelor degree in Physics from the Universidade Federal do Rio de Janeiro-UFRJ, a M.Sc. degree in Geology from UFRJ and a Ph.D. in Geophysics from the University of Edinburgh (UK). Works in Applied Geophysics using electromagnetic methods.